Analytical Methods

ROYAL SOCIETY OF CHEMISTRY

PAPER

View Article Online
View Journal | View Issue



Cite this: *Anal. Methods*, 2023, **15**, 171

# Fabrication of ionic liquid-mesoporous silica/platinum electrode with high hydroelectric stability for electric-field-assisted particle separation

Ruilin Yang,†[a] Lu Liu,†[b] Han Yeong Kaw,[c] Minshu Li,[d] Ji Man Kim,[e] Donghao Li,[ab] Cuicui Liu,[b] Meihua Dong*[b] and Mingshi Jin*[ab]

Received 23rd September 2022
Accepted 28th November 2022

DOI: 10.1039/d2ay01546c

rsc.li/methods

Surface chemistry of electrodes plays a critical role in the fields of electrochemistry and electric-field-assisted separation. In this study, making ingenious use of the ordered mesoporous structure of silica materials and the electrochemical stability of ionic liquids (ILs) when integrated with polyvinylpyrrolidone (PVP), the PVP-modified IL-mesoporous silica/platinum wire (Pt/PVP@meso-$SiO_2$@IL) was fabricated to increase hydroelectric stability and avoid the problem of electrode polarization. The effect of different amounts of mesoporous silica material used to modify the surface of the Pt electrode was systematically investigated. As a result, we successfully obtained a highly ordered mesoporous Pt/PVP@meso-$SiO_2$ material with smooth surface. Because pentyl triethylamine bis(trifluoromethylsulfonyl) imide exhibits a wide electrochemical window between −3 to 3 V, this IL was chosen to modify mesopores under vacuum. Even after repeatedly applying electric field on Pt/PVP@meso-$SiO_2$@IL 100 times, this working electrode remained stable and showed high hydroelectric stability. After verifying the feasibility of this method, it was successfully applied in the electric-field-assisted separation of 2.0 and 3.0 μm polystyrene particles without any impediment from electrode polarization problems. This work provides a brand-new insight for resolving the problem of electrode polarization by developing a versatile tool for the electroseparation of micro-objects.



## 1. Introduction

Electrophoresis has proven to be a valuable technique for the preparation and separation of micro-objects. However, the instability of electrodes is still a great challenge that needs to be tackled urgently because it leads to the frequent formation of gas bubbles throughout the electrophoresis process, especially when the electrode directly comes into contact with the mobile phase, which results in poor target resolution and affects the performance of follow-up detection.[1,2] Several conventional methods that involve isolating the electrode from the solution have been proposed to reduce this limitation.[3–7] In order to drive the vigorous development of electrophoresis technology, it is necessary to make use of the electrode surface interface for separation and improve the stability of the electrode in the solution.

Surface science of electrodes plays a pivotal role in the fields of electrocatalysis, electrochemical sensing, metal corrosion protection, micro-object separation, *etc.*[8,9] The phenomenon of electrode polarization commonly occurs on the electrode surface and may induce electrochemical reactions,[10–12] hence affecting the performance of subsequent separation and analysis. The occurrence of electrode polarization around the electrode can be eliminated by the vigorous stirring of the solution or conducting the process under high flow rates.[13,14] Yet, chemical polarization generated at the electrode surface can be persistent. To overcome this phenomenon, choosing a specific material containing functional groups with high electrode potential for electrode surface modification might be an effective way that can prevent the occurrence of electrochemical reactions. Nonetheless, there are limited reports on the stability of electrodes modified with functional materials.[15,16] Electrode stability mainly depends on the interface of the electrode substrate. In order to broaden the application prospects of modified electrodes in different fields without the occurrence of polarization, the synthesis, characterization and evaluation of the material used to modify the electrode surface are urgently needed.

[a]*Interdisciplinary Program of Biological Functional Molecules, College of IntegrationScience, Yanbian University, Park Road 977, Yanji City, Jilin Province, 133002, PR China*

[b]*Department of Chemistry, Yanbian University, Park Road 977, Yanji City, Jilin Province, 133002, PR China. E-mail: mhdong@ybu.edu.cn; msjin1231@ybu.edu.cn*

[c]*Department of Environmental Science, Zhejiang University, Hangzhou, 310058, PR China*

[d]*Natural Product Research Institute, College of Pharmacy, Seoul National University, Seoul 08826, Korea*

[e]*Department of Chemistry, Sungkyunkwan University, Suwon, 440-746, Republic of Korea*

† Ruilin Yang and Lu Liu contributed equally.

Among the variety of metal-derived electrode materials, bare platinum itself is a suitable electrode due to its high conductivity,[17–19] however, platinum wire easily produces gas bubbles if the potential is highly positive or negative. To solve this problem, several methods that enable the immobilization of functional materials on metallic surfaces have been developed thus far. In particular, polyvinylpyrrolidone (PVP)[20–22] has shown distinguished film-forming properties and dispersibility, and the high electron cloud density on its ring can be complexed with many metal atoms, due to which it can be regarded as a protecting agent under solvothermal conditions. Multiple studies have proven that mesoporous silica material can be successfully modified on the platinum surface *via* PVP,[23] indicating that employing PVP is an ideal strategy for modifying the platinum substrate with functional materials. Ordered mesoporous materials have aroused substantial interest among researchers for application in various fields due to their advantages, such as highly ordered pores, high specific surface area and large pore volume.[24–26] Among these, mesoporous silica materials have been extensively studied in light of their unique biocompatibility and nanostructures, which are suitable for electrocatalysis.[27–30] Ionic liquids (IL) are a kind of electrolytes composed entirely of ions, which render a number of prominent physicochemical properties, including good conductivity, non-volatility and a wide electrochemical window, for various electrochemical applications.[31–35] Therefore, it is hypothesized that filling the three-dimensional mesopores of silica material with high-electrode-potential IL might be beneficial to decrease or even avoid the occurrence of electrode polarization.

Based on the hypothesis mentioned above, in this study, a PVP-stabilized Pt wire modified with ionic liquid-mesoporous silica was fabricated for the first time to avoid electrode reactions that impede the application of conventional electrode materials. In order to increase the electrochemical window of this electrode in water, the electrochemical properties of the IL-modified electrode were evaluated. The stability of the material modified with ionic liquid-mesoporous silica and its application in the electroseparation of micro-particles were also systematically examined.

## 2. Materials and methods

### 2.1 Materials and reagents

The silica precursor [tetraethoxyorthosilicate (TEOS); 99.999%], non-ionic surfactant F-127, polyvinylpyrrolidone (PVP, $M_w = 24\,000$) and pentyl triethylamine bis(trifluoromethylsulfonyl) imide were purchased from Sigma-Aldrich (Bellefonte, PA, USA). The platinum wire was purchased from the Tianjin Lu Cheng metal processing factory (Tianjin, China). NaOH, HCl, $H_2SO_4$, ethanol, and $H_2O_2$ were purchased from Sanfu Chemical Reagent Agency (Yanji, China). Polystyrene particles of different sizes (2.0 and 3.0 μm) were purchased from Aladdin.

### 2.2 Instruments

The dipping-and-pulling machine was purchased from Shanghai Huotong Experimental Instrument Co., Ltd. The syringe pump was obtained from Baoding Rongbai Constant Flow Pump Manufacturing Co., Ltd. A magnetic stirrer was purchased from LNB Instruments. The scanning electron microscopy (SEM) images were obtained by using a Hitachi UHR S 5500 FE-SEM operating at an accelerating voltage of 30 kV. The X-ray diffraction (XRD) patterns were obtained in the reflection mode using a Rigaku D/MAX-2200 Ultima equipped with Cu $K_\alpha$ radiation at 30 kV and 40 mA. The transmission electron microscopy (TEM) images were obtained using a JEOL JEM 3010 at an accelerating voltage of 300 kV. Cyclic voltammetry (CV) was performed on an instrument obtained from Tianjin Lanli Chemical Electronic High Technology Co., Ltd. The process of particle separation was observed under a microscope (Olympus IX 83), and the particles were detected by a UV detector (Agilent 1260 Infinity) based on UV absorbance at 254 nm.

### 2.3 Electrode fabrication

**2.3.1 The pretreatment of the platinum wire.** The preparation of the Pt/PVP@meso-$SiO_2$@IL electrode is shown in Fig. 1. The platinum wire was calcined at 600 °C for 6 hours to oxidize the surface before modification with mesoporous materials. The platinum wire was successively sonicated with 1 M NaOH, deionized water, 1 M HCl and deionized water for 30, 20, 30 and 20 min, respectively, to wash the impurities on the surface. Then, the platinum wire was blow-dried, followed by immersion in the piranha solution ($H_2SO_4 : H_2O_2 = 7 : 3$) for 20 min for hydroxylation. Then, the platinum wire was rinsed with deionized water three times and blow-dried. These pretreatment procedures were carried out to ensure the uniform modification of the platinum surface with the mesoporous material. After that, the platinum wire was rinsed with neutral deionized water and dried in a baking oven at 80 °C.

**2.3.2 Preparation and modification of polypyrrolidone.** Different amounts (0.0122, 0.0366 and 0.0610 g) of PVP were respectively dissolved in 2 g ethanol and sonicated for 30 min. After that, a treated platinum wire was immersed into each PVP solution for 10 min for modification. The modified Pt/PVP samples were dried at 80 °C for 12 h.

**2.3.3 Synthesis and modification of mesoporous silica material.** The synthesis of the mesoporous silica material was carried out by using the sol–gel method. In brief, F-127 was dissolved in absolute ethanol and stirred at 300 rpm for half an hour. After that, TEOS and 0.8 M HCl were added drop by drop into the solution and stirred (400 rpm) at 25 °C for 20 h under a controlled relative humidity of below 20%. To modify the PVP-coated Pt wires, they were immersed into the mesoporous silica solution by using a dipping-and-pulling machine for 5 min. The dipping speed and pulling speeds were set at 2000 μL $s^{-1}$ and 300 μm $s^{-1}$, respectively. The obtained modified Pt wires were then calcinated at 400 °C for 3 h to remove the surfactant F-127.

**2.3.4 Modification of ionic liquid.** In order to avoid polarization of the electrode and production of gas bubbles, the selected ionic liquid, namely pentyl triethylamine bis(trifluoromethylsulfonyl) imide, was immobilized into the mesopores under vacuum for 20 min to fabricate the Pt/PVP@meso-

 

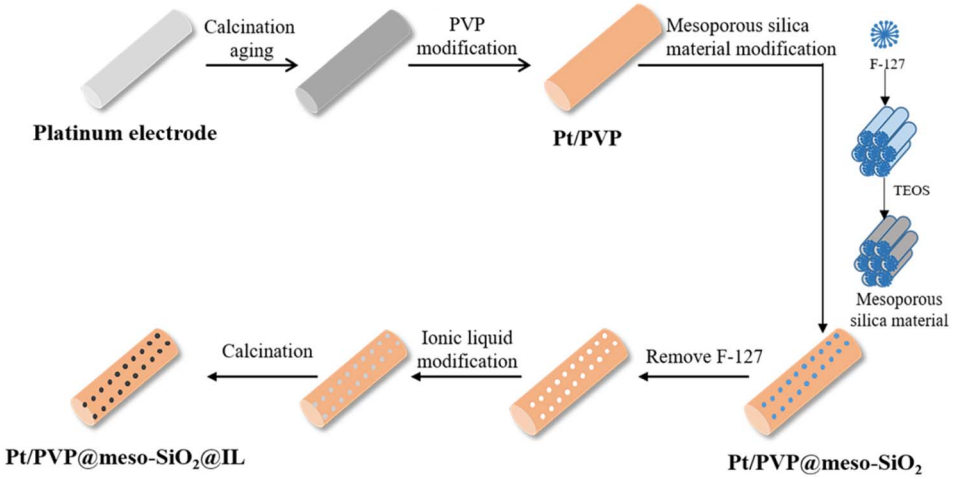


Fig. 1 The flow chart of the fabrication procedure of the Pt/PVP@meso-$SiO_2$@IL electrode.

$SiO_2$@IL electrode. Then, the modified electrode was placed in an 80 °C oven for the immobilization of IL.

### 2.4 Microchip fabrication

The electric-field separation microchip was fabricated by wire imprinting. Three platinum wires (200 μm in diameter) were placed on a cyclic olefin copolymer (COC) plate and sandwiched between two glass microslides using four small binder clips. Then, the COC chip was heated at 127 °C for 20 minutes and then cooled down to room temperature. The wires were then carefully pulled away. Then, two platinum wires modified with the ionic liquid and mesoporous silica material were embedded at both sides of the channel; the resulting channel plate and another COC plate previously drilled with two holes were dried and assembled together with the holes aligned along the channel, sandwiched between two glass microslides, and clamped using binder clips.

## 3. Results and discussion

### 3.1 Characterization of the modified materials

**3.1.1 Effects of different silica content.** The surface-modifying mesoporous material plays significant roles not only in generating an electrode surface with evenly distributed functional groups, but also acts as the main carrier for IL immobilization to prevent direct contact between the ions in water and the electrode surface, which causes the electrode reaction. In this regard, the pore size and pore structure of mesoporous materials can affect the conductivity rate and extravasation rate of ILs. Different contents of TEOS (Table 1) were optimized herein, and the results are shown in Fig. 2. In the presence of 1.0 g TEOS, 0.4 g F-127, 0.4 g 0.8 M HCl and 5.0 g EtOH, the low-angle XRD pattern showed a narrow and well-defined peak, representing a uniform pore structure (Fig. 2a). Despite the fact that the silica content gradually increased with the increase in TEOS amount, the electrode surface began to deteriorate and became unstable, which eventually led to the detachment of silica material from the substrate surface, resulting in a decrease in silica content when TEOS was 2.0 g. Therefore, 1.0 g of silica-modified mesoporous material was selected as the carrier for the subsequent modification of IL.

**3.1.2 Effect of modification time.** The duration of the modification reaction directly affects the amount of mesoporous silica material deposited on the Pt wire surface. Fig. 3a shows the homogeneous formation of mesoporous silica material *via* PVP on the Pt wire electrode without peeling off at the modification time of 5 min. With an increase in modification time, the detachment frequency of mesoporous silica material from the Pt wire surface concurrently increased, as shown in Fig. 3b–d, and cracks were observed when the surface was modified for 30 min. The detachment of the mesoporous silica materials is attributed to the increased thickness due to prolonged modification time, which decreases the stability of the interactions between the mesoporous silica material and the Pt wire surface at the interface. Therefore, the modification time of 5 min was chosen in subsequent experiments. Fig. 3e shows the SEM-EDS mapping of Pt/PVP@meso-$SiO_2$ when modified for 5 min, and the insets denote the even distribution of platinum, oxygen and silica elements on the Pt/PVP@meso-$SiO_2$ surface, which lays the foundation for further modification with IL to increase the working voltage and decrease or avoid electrode polarization.

**3.1.3 The direct electrochemistry of Pt/PVP@meso-$SiO_2$@IL.** In order to increase the working voltage and surface stability of the electrode, pentyl triethylamine

Table 1 The different silica contents employed in the sol–gel method

| Sample number | TEOS (g) | F127 (g) | HCl (g) | EtOH (g) | Si[a] (wt%) |
|---|---|---|---|---|---|
| Pt-1 | 1.0 | 0.4 | 0.4 | 5.0 | 8.34 |
| Pt-2 | 1.5 | 0.4 | 0.4 | 5.0 | 13.64 |
| Pt-3 | 2.0 | 0.4 | 0.4 | 5.0 | 0.2 |

[a] Surface Si refers to the ratio of Si content to the total element ratio calculated from the SEM-EDX results.

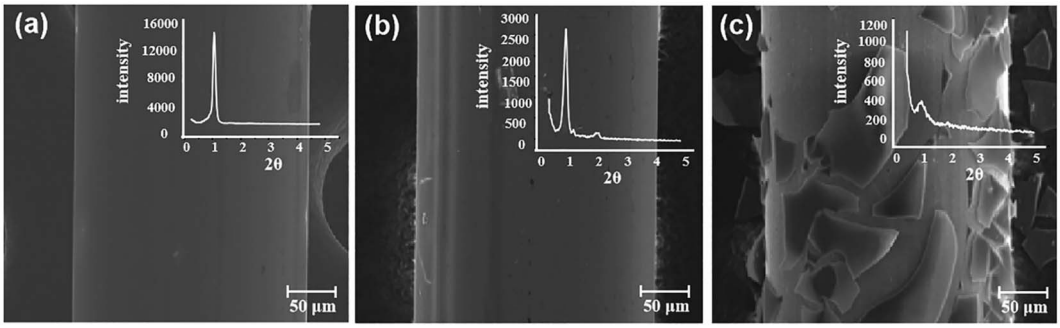


Fig. 2 The SEM images of the effects of modifying the platinum wire with (a) 1.0 g, (b) 1.5 g and (c) 2.0 g of TEOS. The insets show the XRD results under different conditions.

bis(trifluoromethylsulfonyl) imide was chosen to fill the mesopores under vacuum conditions. The results from the XRD analysis, as indicated in Fig. 4a, showed a high small-angle diffraction peak before IL modification, signifying that highly ordered mesopores were synthesized *via* PVP. The peak intensity significantly decreased after modifying with pentyl triethylamine bis(trifluoromethylsulfonyl) imide, suggesting that IL was successfully integrated into the mesopores. Besides, we used electrochemical impedance spectroscopy (EIS) to verify the electrochemical properties of the electrode. As shown in Fig. 4b, the kinetics of electron transfer, which is represented by the impedance values, in the platinum wire before and after modification with mesoporous silica and ionic liquid were in the following order: Pt < Pt/PVP@meso-$SiO_2$ < Pt/PVP@meso-$SiO_2$@IL. The results also recorded an increase in impedance value and a decrease in conductivity after coating the Pt wire with the ionic liquid. The electrochemical properties of the bare platinum wire and the successful fabrication of the Pt/PVP@meso-$SiO_2$@IL electrode were further verified by cyclic voltammetry. As shown in Fig. 4c and d, the oxidation peak of water was visible in the pattern of the platinum wire without functional material modifications. In contrast, there were no oxidation and reduction peaks after the modification of mesopores with the selected IL. Considering that pentyl triethylamine bis(trifluoromethylsulfonyl) imide exhibits a wide electrochemical window, the fact that oxidation and reduction reactions did not occur within the range of −3 to 3 V demonstrates that IL could successfully prevent the occurrence of electrode reactions at the electrode surface in solution. Based on these findings, we can reasonably conclude that the effectiveness of IL in increasing the surface stability of the electrode and avoiding chemical reactions at the electrode is justified.

**3.1.4 Hydroelectric stability of the modified electrode.** Most electrodes are unstable under hydroelectric conditions because of the easy formation of numerous ions that facilitate various reactions at the substrate surface, thus causing the materials deposited on the modified electrode surface to peel off. In this study, the stability of the fabricated Pt/PVP@meso-$SiO_2$@IL electrode was verified by repeatedly applying an electric field on this electrode over 100 cycles and characterizing it by SEM. As displayed in Fig. 4e, the electrode surface remained fully intact without cracks or detachment, which validated the robustness of the modified electrode. This observation can be attributed to the high oxidation and reduction potentials of IL,

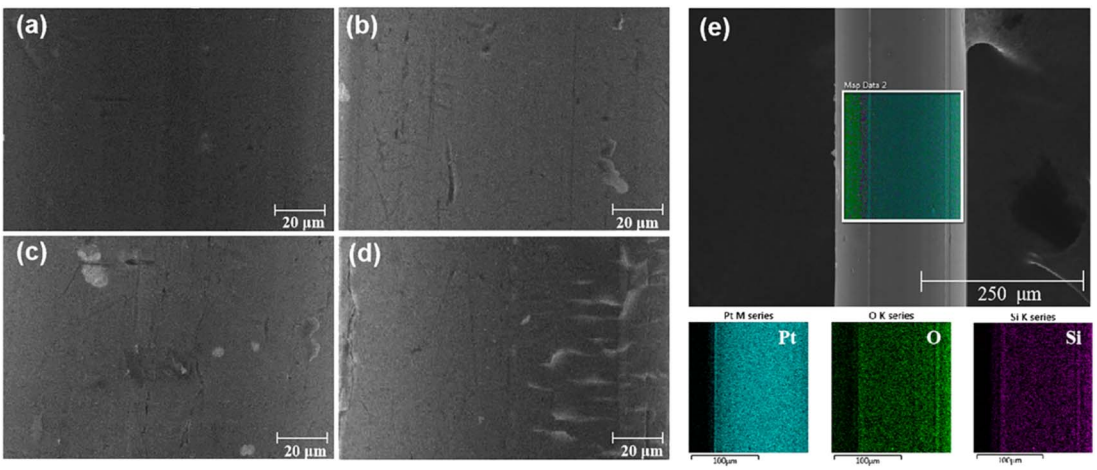


Fig. 3 The SEM images of Pt wire surfaces after modification with mesoporous silica material for (a) 5 min, (b) 10 min, (c) 20 min and (d) 30 min, respectively, while (e) demonstrates the uniform distribution of different elements in the SEM-EDS mapping of the Pt wire modified for 5 min.

 

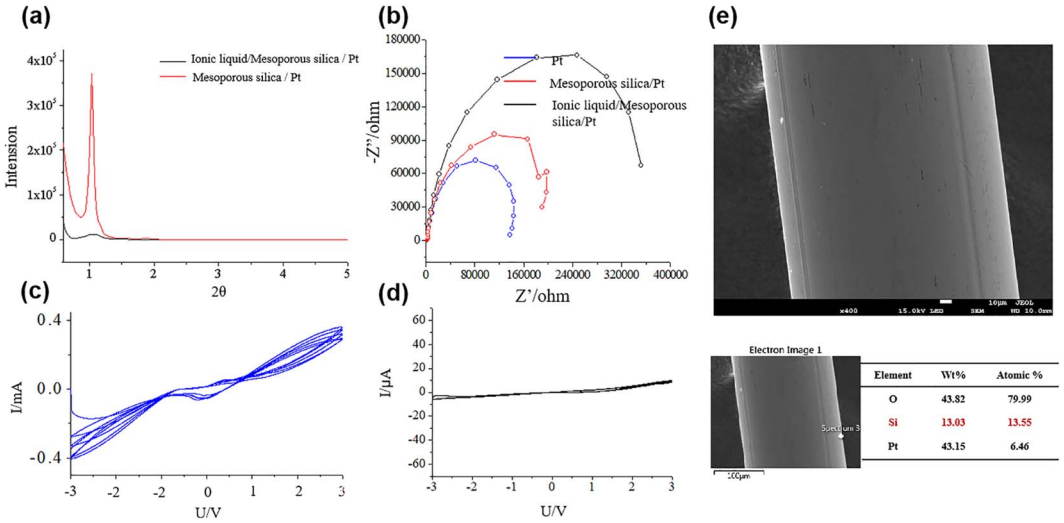


Fig. 4 (a) The XRD analysis of Pt/PVP@meso-$SiO_2$ before and after modification with IL. (b) Electrochemical impedance spectra (EIS) of Pt, Pt/PVP@meso-SiO2, and Pt/PVP@meso-$SiO_2$@IL obtained in 0.1 M KCl containing 5 mM $Fe(CN)_6^{3-/4-}$ (1 : 1). (c) shows the redox peak of the platinum wire detected by CV. The reference electrode was Ag/AgCl, the counter electrode was Pt, the working electrode was Pt, the scan range was between −3 to 3 V, the scan rate was 0.5 V $s^{-1}$, and the electrolyte was deionized water. (d) The CV graph of the functionally modified Pt/PVP@meso-$SiO_2$@IL electrode; the reference electrode was Ag/AgCl, the counter electrode was platinum, the working electrode was Pt/PVP@meso-$SiO_2$@IL, the scan range was between −3 to 3 V, the scan rate was 0.5 V $s^{-1}$, and the electrolyte was deionized water. (e) The SEM images of the working electrode after applying an electric field 100 times.

which hinder chemical reactions from occurring at the electrode surface.

### 3.2 Application

In this paper, the fabrication of Pt/PVP@meso-$SiO_2$@IL provides an innovative approach in the field of electrode preparation to avoid the occurrence of chemical reactions in the electrophoresis system and achieve high stability. A microchip was fabricated to observe the state of the electrode *via* a microscope. A separation channel was constructed by using two Pt/PVP@meso-$SiO_2$@IL electrodes, and deionized water was used as the mobile phase. Under an alternating current of −3 to 3 V in deionized water, gas bubbles were generated in the separation channel when the bare platinum electrode without modification was used (Fig. 5a and b), while none was observed in the separation channel with the Pt/PVP@meso-$SiO_2$@IL electrodes under the same experimental conditions (Fig. 5c and d). The electroseparation chip consisted of two Pt/PVP@meso-$SiO_2$@IL electrodes (Fig. 6a). As shown in Fig. 6b, particles at a high concentration were evenly dispersed in the separation channel. In order to ensure that all particles start at the same electrode surface position, the parameters $U = 3.0$ V, $f = 0.1$ Hz, and duty cycle value = 99% were applied. All the particles tended to align in one line after electro-focusing (Fig. 6c). The same phenomenon was observed under a low particle concentration as well (Fig. 6d and e). From the above findings, we can conclude that the Pt/PVP@meso-$SiO_2$@IL electrode has high stability, which was favorable for the study of the electrical field and the electrical separation behavior of the target.

Subsequently, we applied this functional material in micro-object separation to verify its practicality. The separation behavior was similar to the separation mode employed in traditional electric field-flow fractionation (EIFFF),[36] as shown in Fig. 7a. EIFFF is a sub-technique of field-flow fractionation, which realizes the separation of target particles (such as cells, particles, and proteins) based on the electrophoretic mobility and size of the analytes by using a constant direct current (DC) field or alternating current (AC) field. The movement behavior of the micro-objects (polystyrene particles) was observed by using a microscope, and the separation system is illustrated in Fig. 7b. Before initiating the separation process, the 2.0 and 3.0 μm particles were injected into the microchip and the mobile phase was halted. These two types of particles remained focussed on one side of the electrodes under the following electrical parameters: pulse voltage of 3.0 V, pulse frequency of 0.1 Hz and duty cycle (dc) values of 99%. The separation began with the application of an alternating current with the electrical parameters 3.0 V, 2.0 Hz and dc = 50%. The two particles migrated in a zig-zag motion within the separation channel and were ultimately separated (Fig. 7c). The microchip was directly connected to a UV detector, which verified that the mixed particles with different sizes could not be separated when there was no electric field. With the Pt/PVP@meso-$SiO_2$@IL electrode, the applied voltage could achieve complete separation, and the results obtained from SEM characterization also indicated good separation performance for 2.0 and 3.0 μm particles (Fig. 7d). From these results, it can be deduced that the Pt/PVP@meso-$SiO_2$@IL electrode exhibits high hydro-electric stability in water, thus proving its broad applicational prospect in the area of micro-object separation science, and this functionality will play a significant role in electrochemistry, anti-corrosion industry, *etc.*

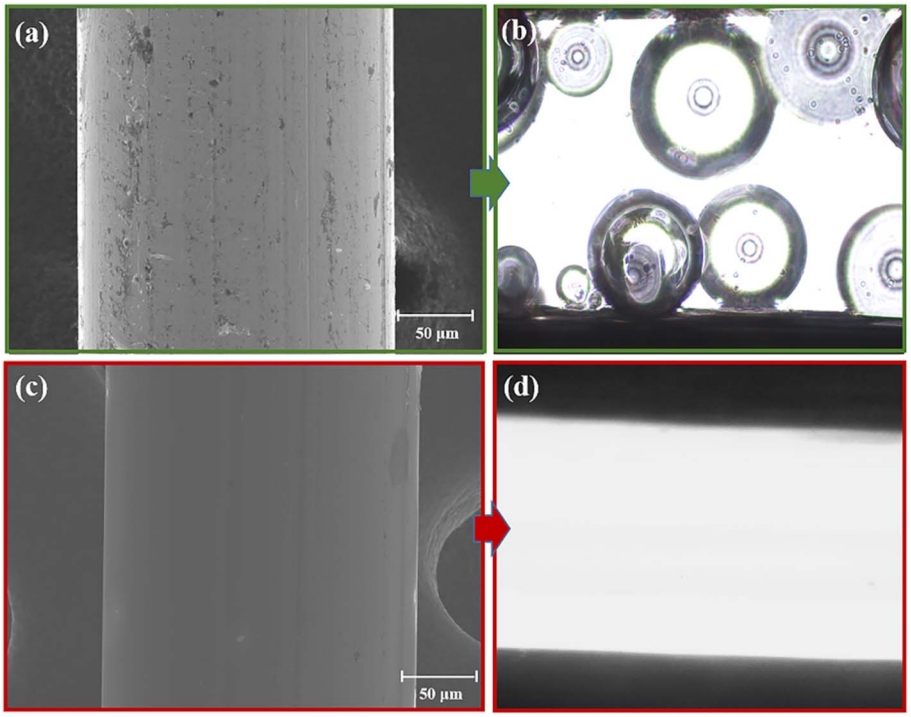


Fig. 5 (a) The SEM image of the bare platinum wire. (b) The microscopic image shows the formation of gas bubbles within the separation channel while using bare platinum wires as electrodes. (c) The SEM image of Pt/PVP@meso-$SiO_2$@IL. (d) The separation channel without gas bubbles while using Pt/PVP@meso-$SiO_2$@IL electrodes under the same alternating current of −3 to 3 V in deionized water.

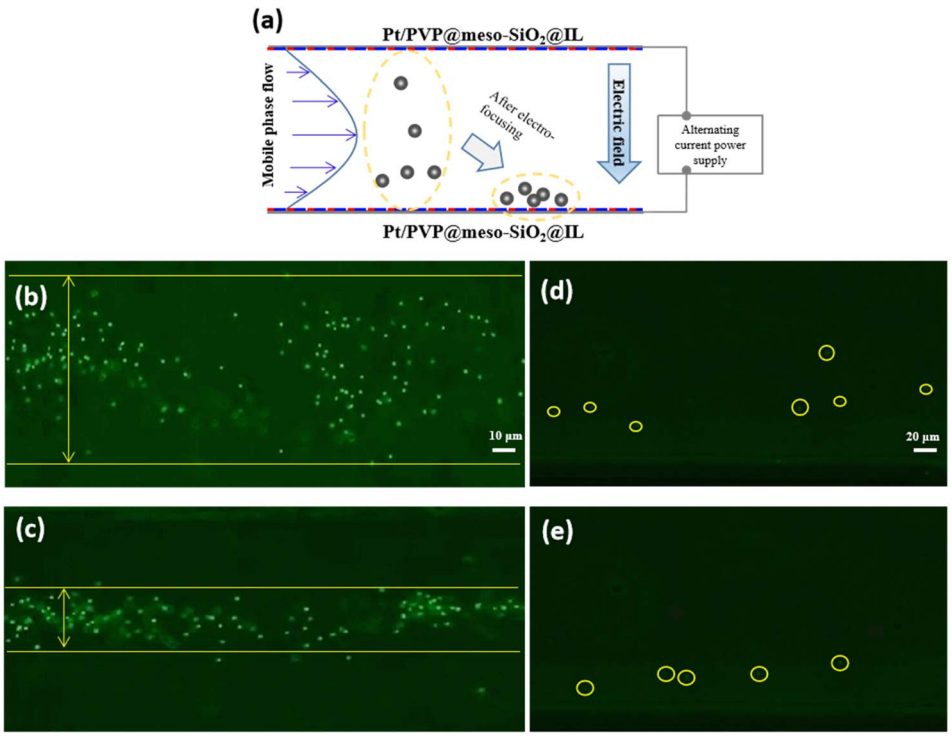


Fig. 6 (a) The electrophoresis chip used for particle focusing under the electric field. (b) and (c) show high-concentration 2.0 μm PS before and after electro-focusing. (d) and (e) show low-concentration 2.0 μm PS before and after electro-focusing. The electrical parameters were $U$ = 3.0 V, $f$ = 0.1 Hz, and duty cycle value = 99%.

 

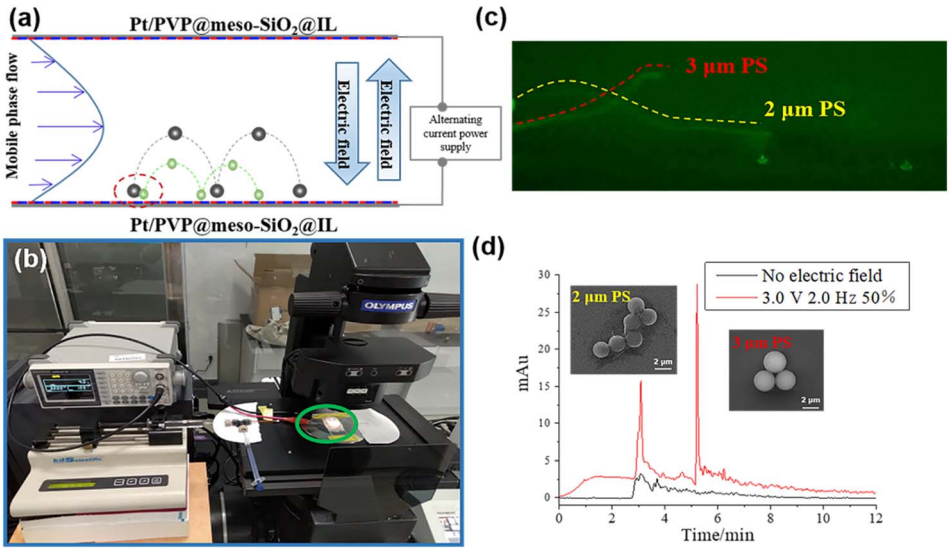


Fig. 7 (a) The traditional EIFFF separation mechanism while employing Pt/PVP@meso-$SiO_2$@IL as the electrodes. (b) Photograph showing the installation of the separation system connected to a microscope to observe the movement behavior of micro-objects (polystyrene particles) in real time. (c) The 2.0 μm and 3.0 μm polystyrene particles were successfully separated under an alternating current with the electrical parameters of 3 V, 2.0 Hz and dc = 50%; the mobile phase was deionized water, and two Pt/PVP@meso-$SiO_2$@IL wires were used as the electrodes. (d) The mixed particles were separated in the fabricated microchip and directly detected by a UV detector, and the insets show the SEM images of the separated fractions.

## 4. Conclusions

In summary, a unique hydroelectric electrode termed Pt/PVP@meso-$SiO_2$@IL with excellent electrical properties that prevent the occurrence of electrochemical reactions was successfully fabricated in this study. This functional Pt/PVP@meso-$SiO_2$@IL electrode could achieve simultaneous microparticle separation with high electrode stability, thereby solving the gas bubble formation problem in traditional electric-field flow fractionation and the impediment caused by electrode polarization. Furthermore, this modification method is simple, and the fabricated material showed high surface and electrochemical stabilities, thus laying the foundation for further research in the realms of micro-object electro-separation, material preparation, corrosion prevention in electrode materials and interfacial reactions.

## Author contributions

Ruilin Yang: investigation, writing – review & editing. Liu Lu: investigation, writing – original draft, writing – review & editing. Han Yeong Kaw: investigation, methodology. Minshu Li: supervision. Ji Man Kim: writing – review & editing, supervision. Donghao Li: supervision. Cuicui Liu: writing and methodology. Meihua Dong: supervision, writing – review & editing. Mingshi Jin: supervision, writing – review & editing.

## Conflicts of interest

The authors declare that they have no known competing financial interests or personal relationships that could have appeared to influence the work reported in this paper.

## Acknowledgements

This study was supported by grants from the National Natural Science Foundation of China (No. 22104127, 22176164, 21775134) and Higher Education Discipline Innovation Project (111 Project, No. D18012).

## References

1 A. N. Ivanovskaya, A. M. Belle, A. M. Yorita, F. Qian, S. Chen, A. Tooker, R. G. Lozada, D. Dahlquist and V. Tolosa, *J. Electrochem. Soc.*, 2018, **165**, G3125–G3132.
2 J. H. Han, J. Jang, B. K. Kim, H. N. Choi and W.-Y. Lee, *J. Electroanal. Chem.*, 2011, **660**, 101–107.
3 M. C. Buzzeo, C. Hardacre and R. G. Compton, *ChemPhysChem*, 2006, **7**, 176–180.
4 Y. Wang, X. Yu, Y. Liu and Q. Wang, *Phys. Chem. Chem. Phys.*, 2018, **21**, 217–223.
5 J. Gao, R. Riahi, M. L. Sin, S. Zhang and P. K. Wong, *Analyst*, 2012, **137**, 5215–5221.
6 D. Li, W. Yu, T. Zhou, M. Li, Y. Song and D. Li, *Analyst*, 2022, **147**, 1106–1116.
7 Z. Zhang, Y. Luo, X. Nie, D. Yu and X. Xing, *Analyst*, 2020, **145**, 5603–5614.
8 L. Coustan, K. Zaghib and D. Bélanger, *J. Power Sources*, 2018, **399**, 299–303.
9 B. K. Gale and M. Srinivas, *Electrophoresis*, 2005, **26**, 1623–1632.
10 H. Chun, *J. Chromatogr. A*, 2018, **1572**, 179–186.
11 M. D'Amours and D. Belanger, *J. Phys. Chem. B*, 2003, **107**, 4811–4817.

12 R. P. Kalakodimi and M. Nookala, *Anal. Chem.*, 2002, **74**, 5531–5537.
13 S. Y. Moon, B. Naik, C.-H. Jung, K. Qadir and J. Y. Park, *Catal. Today*, 2016, **265**, 245–253.
14 S. S. Moganty, R. E. Baltus and D. Roy, *Chem. Phys. Lett.*, 2009, **483**, 90–94.
15 P. Zhou, L. Yao and B. Su, *ACS Appl. Mater. Interfaces*, 2020, **12**, 4143–4149.
16 K. J. Lin, L. J. Chen, M. R. Prasad and C. Y. Cheng, *Adv. Mater.*, 2004, **16**, 1845–1849.
17 I. Pastoriza-Santos and L. M. Liz-Marzan, *Langmuir*, 2002, **18**, 2888–2894.
18 X. Li, C. Hao and Q. Lei, *Mater. Res. Bull.*, 2012, **47**, 352–355.
19 H. Song, R. M. Rioux, J. D. Hoefelmeyer, R. Komor, K. Niesz, M. Grass, P. D. Yang and G. A. Somorjai, *J. Am. Chem. Soc.*, 2006, **128**, 3027–3037.
20 Z. Liu, O. Terasaki, T. Ohsuna, K. Hiraga, H. J. Shin and R. Ryoo, *ChemPhysChem*, 2001, **2**, 229–231.
21 P. Singh, H. Singh, V. Castro-Aceituno, S. Ahn, Y. J. Kim, M. E.-A. Farh and D. C. Yang, *J. Nanopart. Res.*, 2017, **19**, 995–1003.
22 A. Wang, Y. Yang, Y. Qi, W. Qi, J. Fei, H. Ma, J. Zhao, W. Cui and J. Li, *ACS Appl. Mater. Interfaces*, 2016, **8**, 8900–8907.
23 U. H. Lee, J.-H. Yang, H.-j. Lee, J.-Y. Park, K.-R. Lee and Y.-U. Kwon, *J. Mater. Chem.*, 2008, **18**, 1881–1888.
24 J. M. Kim, S. Jun and R. Ryoo, *J. Phys. Chem. B*, 1999, **103**, 6200–6205.
25 Y. Jung, R. L. Spray, J. H. Kim, J. M. Kim and K. S. Choi, *Chem. Commun.*, 2010, **46**, 6566–6568.
26 S. H. Joo, J. Y. Park, C. K. Tsung, Y. Yamada, P. Yang and G. A. Somorjai, *Nat. Mater.*, 2009, **8**, 126–131.
27 S. Doblinger, T. J. Donati and D. S. Silvester, *J. Phys. Chem. C*, 2020, **124**, 20309–20319.
28 P. Wang, S. M. Zakeeruddin, P. Comte, I. Exnar and M. Gratzel, *J. Am. Chem. Soc.*, 2003, **125**, 1166–1167.
29 N. Terasawa and K. Asaka, *Sens. Actuators, B*, 2014, **193**, 851–856.
30 B. Barik, A. Kumar, P. S. Nayak, L. S. K. Achary, L. Rout and P. Dash, *Mater. Chem. Phys.*, 2020, **239**, 122028.
31 H. Shim, C. Gyun Shin, C.-J. Heo, S.-J. Jeon, H. Jin, J. Woo Kim, Y. Jin, S. Lee, J. Lim, M. Gyu Han and J.-K. Lee, *Appl. Phys. Lett.*, 2014, **104**, 051104.
32 M. Ornthai, A. Siripinyanond and B. K. Gale, *Anal. Chem.*, 2016, **88**, 1794–1803.
33 B. K. Gale, K. D. Caldwell and A. B. Frazier, *IEEE Trans. Biomed. Eng.*, 1998, **45**, 1459–1469.
34 M. Sun, P. Agarwal, S. Zhao, Y. Zhao, X. Lu and X. He, *Anal. Chem.*, 2016, **88**, 8264–8271.
35 T. K. Mudalige, H. Qu, D. Van Haute, S. M. Ansar and S. W. Linder, *TrAC, Trends Anal. Chem.*, 2018, **106**, 202–212.
36 A. L. K. Lao, Y. K. Lee and I. M. Hsing, *Anal. Chem.*, 2004, **76**, 2719–2724.

 